International Journal of Biological Macromolecules 185 (2021) 997–1004

Contents lists available at ScienceDirect

International Journal of Biological Macromolecules

journal homepage: www.elsevier.com/locate/ijbiomac

Janus hybrid sustainable all-cellulose nanofiber sponge for oil-water separation

Aphra Agaba [a], Ifra Marriam [b], Mike Tebyetekerwa [c,*], Wang Yuanhao [a,*]

[a] Hoffmann Institute of Advanced Materials, Shenzhen Polytechnic, 7098 Liuxian Boulevard, Nanshan District, Shenzhen 518055, PR China
[b] School of Mechanical, Medical, and Process Engineering, Faculty of Engineering, Queensland University of Technology, 2 George St, Brisbane, Qld 4000, Australia
[c] School of Engineering, College of Engineering and Computer Science, The Australian National University, Canberra, ACT 2601, Australia

ARTICLE INFO

Keywords:
Janus
Cellulose nanofibers sponge
Oil-water separation

ABSTRACT

Two-faced characteristics and performance of materials driven by asymmetric physical or chemical properties exist in Janus hybrid materials which show synergistic and improved properties for a variety of applications. Here, we report a facile synthesis of Janus hybrid sustainable cellulose nanofibers (CNFs) sponge with asymmetric wettability and strong mechanical property for excellent separation efficiency of oil-water emulsions. Briefly, the CNF Janus hybrid sponge was fabricated by freeze-drying of two separate CNF suspensions into one, each prepared separately by introducing CNFs in methyltrimethoxysilane (MTMS) or 3-glycidoxypropyltrimethoxysilane (GPTMS) for hydrophobic or hydrophilic performance, respectively. The sponge demonstrated satisfactory mechanical stability with an excellent recovery from 80% compressive strain and high pore tortuosity. When employed for oil-water separation, the Janus hybrid sponge could selectively be used to collect water or oil by just switching its side facing the oil-water mixture feed *via* unidirectional gravity-assisted separation, with recyclability. The fabrication of such Janus hybrid sponge is one of the many approaches for utilizing nanofibers in structurally adaptive, self-supported asymmetric membrane structures in a 3D network.

1. Introduction

Materials science and engineering research is strongly driven and inspired by natural materials, organisms, insects, animals and processes existing enormously in nature. For example, cactus, lotus, spider fibers and desert beetles exhibit properties stemming from their asymmetric physical assembly or asymmetric chemical nature, both in bulk and in thinfilms [1–3]. Such materials with multiple-in-one properties are interesting for a variety of engineering applications. Materials fabricated with double-faced behaviors (asymmetric properties) are named Janus with the name coming from Roman god Janus, due to a belief (according to Roman mythology) that Janus is double-faced, with the two faces placed back to back, enabling him to simultaneously see the past and the future [4,5]. In this sense, therefore, Janus hybrid materials can be described as a class of materials with opposing properties on both sides. They can be prepared by asymmetric layers fabrication or asymmetric surface adjustment. The structure of Janus materials allows oppositely-differing material properties at the interface to work together leading to a distinct transport behavior with in the material. The opposite interaction between the different sides of the Janus membrane makes it synergistic and promising in applications such as switchable ion transport, droplet manipulation, bubble aeration, unidirectional oil-water separation, interfacial mass transfer and many others [4–8]. In fluid separation applications, hydrophobic-hydrophilic porous hybrid Janus membranes are fluid management materials with diode-like properties such as unidirectional fluid transport across the porous media allowing one-way flow of liquids with negligible pressures, but capable of opposing it in reverse directions up to very high pressures. This controlled application of the opposite sides of the absorbent porous sponges imparts tunable fluid diodicity, made possible by competing capillary forces.

Focusing on oil-water separation application, recently, there is an increase in the production of oil/water mixtures from both domestic and industrial, [9] such as petroleum, manufacturing, food, steel and many others. Therefore, efficient separation of oil-water mixtures is a prerequisite for a sustainable economy, which is an important challenge requiring fast viable solutions. Indeed, oil spill incidents and/or a combination of oily waste liquids in existing water resources not only disrupts the natural ecosystem balance and intimidate human health but also is a waste of precious resources [10]. Janus membranes can be an

* Corresponding authors at: 32 North Road, Canberra, ACT 2600, Australia (M.T.).
E-mail addresses: mike.tebyetekerwa@anu.edu.au (M. Tebyetekerwa), wangyuanhao@szpt.edu.cn (W. Yuanhao).

https://doi.org/10.1016/j.ijbiomac.2021.07.027
Received 22 February 2021; Received in revised form 1 July 2021; Accepted 1 July 2021
Available online 6 July 2021

efficient solution. This is because traditional existing separation methods [11] for the separation of oil–water mixtures such as gravity separation, membrane separation, air flotation, electro-coalescence, and many others have consistent drawbacks like high cost (energy), low efficiency, additional secondary pollution, complicated mode of application (especially if it is a spill). In addition, they are not capable of separating well stabilized (with surfactants) oil–water mixtures with droplet sizes below 20 μm due to the tendency of the emulsion droplets exhibiting a lower surface energy [12].

The techniques of oil spill clean-up currently employed involve; (1) using dispersing agents to disperse oil phase in water which facilitates natural degradation [13,14], (2) directly burning the floating oil [15,16], and (3) using suitable adsorbents to extract the oil phase from the water surface [17]. Amongst these, the use of adsorbents is economical, efficient and eco-friendly as oil can be properly reclaimed or discarded without any secondary pollution. Functional sorbents made from polymers, graphene, silica aerogels, organophilic clays, carbon nanotubes, nanocellulose have been applied for oil-water separation [17]. However, the absorption efficiency of many these existing absorbents is limited, and come with increased production costs especially for the case of silica aerogels and exfoliated graphite. However, nanocellulose based sorbents stand out. Cellulose is a good candidate material because of many reasons. It is abundant in nature, sustainable and environment friendly [18,19] and thus if employed to fabricate porous highly adsorbent sponge/aerogel materials, it will be cost effective. In the previous past, various research groups reported hydrophobic, flexible, and ultra-light sponges and aerogels from cellulose nanofibers (CNFs) for oil clean-up fabricated *via* octadecyltrichlorosilane modification [20], a silylation process in water [21], freeze-drying and subsequent triethoxy(octyl) silane vapor deposition [22,23] with excellent ultra-high absorption capacity. However, in their reports, the absorption material reuse, oil recovery, structure integrity (mechanical and chemical properties) were key issues especially for all-CNF based materials.

In this work, a facile approach to fabricate a Janus hybrid sustainable all-CNF sponge for oil-water separation is reported. The CNF Janus hybrid sponge with opposing surface wettability and strong mechanical property showed excellent separation efficiency of oil-water emulsions and oil spill removal. Briefly, the CNF Janus hybrid sponge was constructed *via* a frozen hydrophilic CNF membrane with a single side hydrophobic CNF suspension coating. The resultant sponge possessed hierarchical porous structure with low surface energy endowing the hydrophobic side with a water contact angle of up to 156°. The sponge also exhibited satisfactory integrated mechanical and chemical stability properties with a rapid recovery from 80% compression strain and high pore tortuosity.

2. Materials and methods

2.1. Materials

n-Hexane, THF, acetic acid, toluene, dichloromethane, paraffin oil, oil red (an organic dye) sodium dodecyl sulfate (SDS), Methyltrimethoxysilane (MTMS), 3-glycidoxypropyltrimethoxysilane (GPTMS) were all sourced from Aladdin Chemical Reagent Co. Ltd. (China). CNFs were purchased from Tianjin Haojia Cellulose Co., Ltd. (China). Milli-Q deionized water was used in all the experiments. All solvents and reagents were used without further purification.

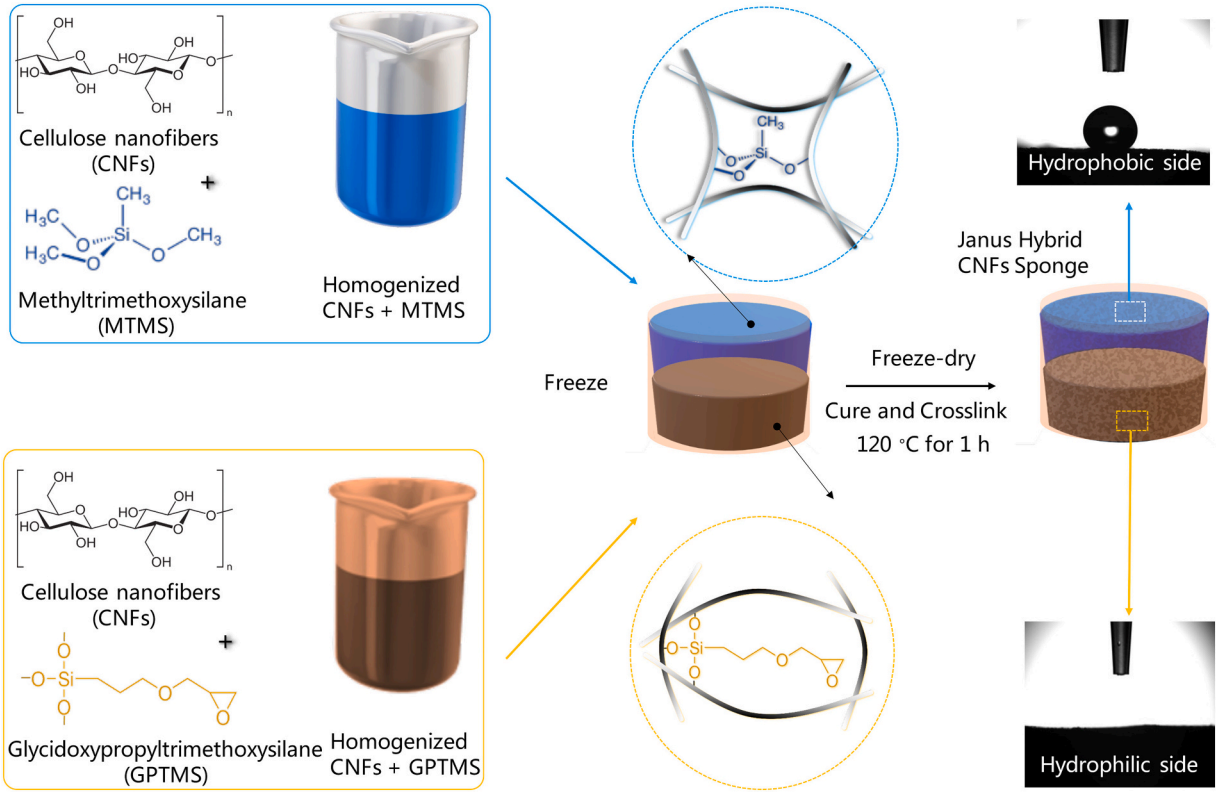

Fig. 1. Preparation of Janus hybrid sustainable all-CNF sponge. The schematic depict the techniques and steps employed to obtain Schematic CNF Janus hybrid sponge. Initial stages involved adding CNFs to MTMS and GPTMS, followed by stirring to obtain their homogenized solutions on opposite sides. The separately prepared homogenized solutions were then frozen into CNF-based dispersions which were later freeze-dried for 48 h and cured at 120 °C for an hour to promote further crosslinking. The final product was a Janus hybrid CNF sponge with asymmetric wettability and strong mechanical properties.

2.2. Methods

2.2.1. Preparation of CNF Janus hybrid sponge

To design Janus hybrid sustainable all-CNF sponge with asymmetric wettability, CNF suspensions were stirred in both Methyltrimethoxysilane (MTMS) and 3-glycidoxypropyltrimethoxysilane (GPTMS) in separate glasses (Fig. 1). The resulting homogeneous mixtures were frozen and then freeze dried. Thereafter, the obtained sponge was further cured and then dried to promote further crosslinking. CNF was chosen as building blocks for making Janus hybrid sponge due to its high aspect ratio and excellent chemical, and barrier properties. MTMS was used as hydrophobic modification reagent to decrease the surface energy of cellulose nanofibers. As a reference, pristine CNF sponge was also prepared by freeze-drying of pristine cellulose nanofibers suspension without any modification. In detail, first CNF suspensions, MTMS and GPTMS solutions were prepared separately. The optimized experimental contents involved CNF suspensions made by adding 24 g of CNFs in 150 g of distilled water, followed by pH adjustment with acetic acid to pH 4. MTMS and GPTMS solutions were made by adding 5.2 g of MTMS or GPTMS in 100 g of water. Then, CNF suspensions were stirred with either MTMS and GPTMS solutions in separate glasses at 500 rpm for 6 h at ambient temperature in water. The resulting homogeneous mixtures were half frozen and then freeze dried at -50 °C on Labconco FD5-3, USA for 48 h. Thereafter, the obtained sponge was further cured and maintained at 120 °C for 1 h to promote further crosslinking. The sponges had good interaction courtesy of the Si-O-Si bonds at the interface, due to the presence both GPTMS and MTMS with Si—O components.

2.2.2. Preparation for oil-water emulsions and separations

Fine oil-water mixtures were prepared by adding some surfactants to the oil-water mixture and then stirring at 300 rpm for 12 h. n-hexane was dyed with oil red before mixing with deionized water to enhance experiment visibility and the mixture was stabilized with SDS. The as-prepared CNF Janus hybrid sponge was clipped into a home-made filtration device of 2 cm in diameter. The oil-water mixture was poured into the glass funnel and the water or oil permeated automatically under the influence of gravity. This procedure was repeated for different types of oil-water mixture separations.

2.2.3. Separation measurements

To calculate the separation flux (F) of collected oil or water, Eq. (1) was employed, where V is the volume of the permeate, A is the valid filtration area of the sponge and T is the testing time.

$$F = V/AT \tag{1}$$

Also, the separation efficiency was calculated by considering the rejection efficiency in percentage (E%) using Eq. (2), where $C_{filtrate}$ and C_{feed} are concentrations of permeate and the original oil-water feed after one-time separation, respectively.

$$E(\%) = 1 - C_{filtrate}/C_{feed} \tag{2}$$

For oil-water absorption capacity measurements, the CNF Janus hybrid sponges were first weighed with the value recorded followed by dipping the sponge in the organic solvent or oil for about 2 min. Organic solvent (oil)-saturated sponges were removed with excess solvent on the surface allowed to drip, and then immediately weighed and value recorded. To determine the mass adsorption capacity (C_a) of the Janus hybrid sponge Eq. (3) was employed, where M_0 is the mass of the sponge before absorption and M_t is the mass of the sponge after absorption, respectively.

$$C_a(\mathrm{g/g}) = \frac{M_t - M_0}{M_0} \tag{3}$$

2.3. Characterization

The surface morphology of the sponges was analysed using scanning electron microscopy (SEM Hitachi TM-3030). All samples were sprayed with a layer of gold prior to the measurements. N_2 adsorption–desorption isotherms were done at 77K °C using V-Sorb 2800P, China porosimetry system. The specific surface areas and pore size distributions were calculated using multipoint Brunauer-Emmett-Teller (BET) method and Barrett–Joyner–Halenda (BJH) method. Fourier transform infrared spectra (FTIR) were done on PerkinElmer Spectrum Two, USA spectrophotometer with a spectral range of 4000–400 cm^{-1} and a step of 4 cm^{-1}. The compressive stress-strain tests were obtained using Changchun Xinke universal testing machine, China equipped with a 50 N loading cell. The thermal stability of the sponges was done on a TG 209 F3 Tars thermogravimetric analysis (TGA) equipment with start sample weight of 20 mg heated from room temperature to 800 °C at a rate of 10 °C/min under nitrogen atmosphere. The surface wettability of the CNF Janus hybrid sponges were evaluated by the static water contact angle (WCA) measurements at 25 °C. The obtained contact angle was analysed using contact angle software which measures the droplet angle from the shape of its image.

3. Results and discussion

3.1. All-CNF sponge characterization

3.1.1. Surface morphology

The morphologies of the CNFs sponges on opposite sides modified with MTMS and GPTMS were observed using SEM, by taking the micrographs of the top and bottom of the self-supporting sponge sample (Fig. 2A). Also, pristine CNFs sponge SEM was captured (Fig. S1). The GPTMS-modified SEM showed numerous and larger pores as compared to MTMS-modified side of the sponge which were smaller in size. Critical observation of GPTMS-modified CNF sponge side in comparison pristine CNF showed various wide pore walls and thin sheets. This is attributed to the aggregation of CNFs during freezing and ice crystal growth, which is responsible for the migration of CNFs around the crystal boundaries [24]. The same mechanism is expected for pristine CNFs. However, we observed numerous nanofibers within the pristine SEM image in addition to the thin sheets. The difference in morphology can be attributed to the open-ended structure (unlike in modified sponge with one being less porous and hydrophobic) which facilitates solvent exchange. The modified sponge also had improved crosslinking due to the GPTMS unlike pristine CNFs, and thus reduced bonding of the nanofibers in pristine CNFs sponge as a result. For MTMS-modified side, a porous structure having thin nanosheets, nanofilaments, and nanoparticles was observed. The nanosheets are attributed to agglomeration of CNFs during the freezing as explained above. The nanoparticles observed in the MTMS-modified side are of silica in MTMS, which also confirms the successful modification CNFs with MTMS. The rough morphology on the MTMS-modified side of the sponge is key to obtaining hydrophobic CNFs. Overall, the modified CNF sponge exhibited a hierarchical 3D open cell geometry interconnected with minor cellular pores, thin sheets, nanoparticles, and nanofilaments. It is also important to note that, without SEM images, both sides of the modified CNF sponges with naked eyes appeared same.

3.1.2. FTIR analysis

The dual surface chemical behavior of the sponges was also characterized by Fourier transform infrared (FTIR) spectroscopy (Fig. 2B). First, neat CNFs sponge showed several peaks in the FTIR spectra at 3345 cm^{-1}, 2920 cm^{-1}, and 1020–1160 cm^{-1} which are ascribed to the -OH, C—H and C—O stretching vibrations [25]. In addition to the identified peaks, both modified sides of the sponge showed extra peaks signifying successful modification of cellulose by MTMS and GPTMS. For example, the spectra of MTMS-modified CNF side of the sponge showed

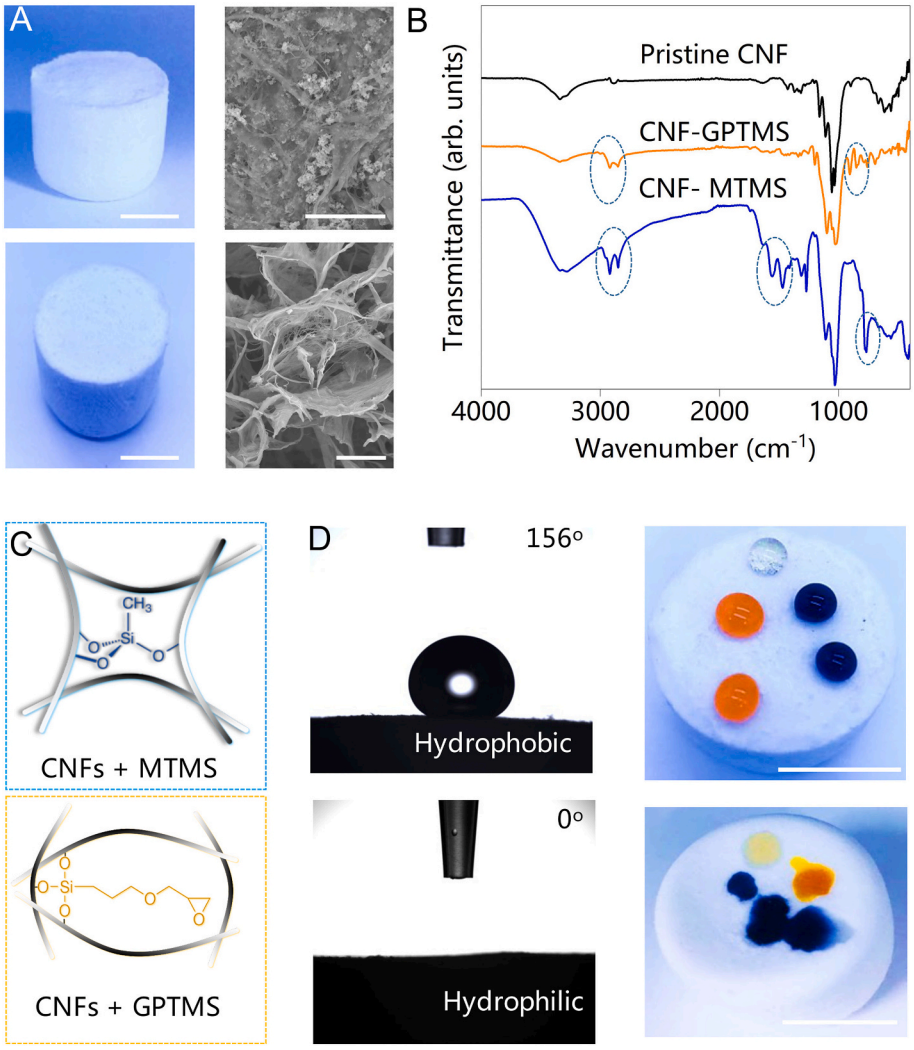

Fig. 2. Chemical and physical properties of Janus hybrid sponge. (A) Photographic images of the two sides of the sponge. Top image depicts the hydrophobic side (MTMS-modified) and bottom is the hydrophilic side (GPTMS-modified) together with the corresponding SEM images in (B). Both sides looked similar when observed using naked human eyes. (C) FTIR spectra of neat CNF and modified-CNF nanosponge sides. (D) Water contact angle and the behavior of the Janus hybrid sponge towards water on hydrophobic and hydrophilic surfaces. The water drops are presented in different colors for clear visibility. All photographic images' scale bars are 1 cm and SEM images scale bars are 25 μm.

new peaks at 766, 2925, and 1273 cm^{-1} which are assigned CH_3 vibrations in silicane, Si–CH_3 bonds, and Si–O–Si bonds, respectively [26,27]. For the case of GPTMS-modified CNF side, the spectra showed two sharp peaks at 904 cm^{-1} and 851 cm^{-1} which are ascribed to the epoxide groups from GPTMS [28] and in addition to the peak at 2925 cm^{-1} from Si-CH_3 bond. Overall, the results confirm existence of covalent bonds and the strong interfacial interactions between cellulose and organosilanes. The strong interfacial interactions are beneficial in many practical applications.

3.1.3. Water contact angle measurements

We also analysed the surface properties of the modified CNF sponge towards liquids. The MTMS-modified side of CNF sponge demonstrated superhydrophobicity, opposite to superhydrophilicity of the GPTMS-modified side (Fig. 2C) when different liquids were introduced on their surfaces. This makes our sponge Janus hybrid due to the asymmetric wettability of the two sides [4,5]. To quantify whether we had a good Janus hybrid CNF sponge, we performed water contact angle measurements (Fig. 2D). For the hydrophilic layer, the water droplet spread rapidly on the sponge surface giving a water contact angle of 0°, attributing the highly porous nature of the sponge. In contrast, the hydrophobic side of the sponge showed a water contact angle of 156° with a round shape retention of the water droplet. This is attributed to successful silane modification. Also, the surface roughness and low surface energy are beneficial in improving the hydrophobicity. In addition, the hydrophobic side of CNF sponge could support water droplets to stand on its surface while the oil droplet could be immediately absorbed. Excellent hydrophilicity usually leads to oleophobicity in a water environment. The water contact angles strongly depend on the functional groups on the adsorbent surfaces. Therefore, in this case, it is likely that MTMS coating induced by the functional groups (such as -Si-O-CH_3–) facilitated the hydrophobicity. Neat CNF is known to be hydrophilic. Therefore, we compared its hydrophilicity with the GPTMS-modified sponge side (Fig. S2). From the results, compared to the GPTMS-modified sponges, CNF hydrophilicity was relatively inferior and generally fragile (Fig. S3) when in contact with water. When the evolution of hydrophilicity with time was measured, neat CNFs water droplet attained a minimum angle of ~5° after 6 s, whereas GPTMS-modified sponges showed a superhydrophilicity with water contact angle of 0° within 3 s.

3.1.4. Mechanical properties

For a material to be employed in the separation of oil-water mixtures it should exhibit some important properties. One of the key property is, it should be shape-stable with proper pore sizes to repel oil, allow water penetration and also avoid fouling [29]. During our experiments, we noted that pristine CNF sponges were fragile and showed a water induced-shape recovery while the Janus hybrid sponges emulated higher flexibility and could be manipulated without breaking. At low compressive strains of 40% (Fig. 3A), both the Janus hybrid and pristine CNF sponge showed similar compressive stress-strain behaviors with three distinct regions. For example, the initial low and linear strain

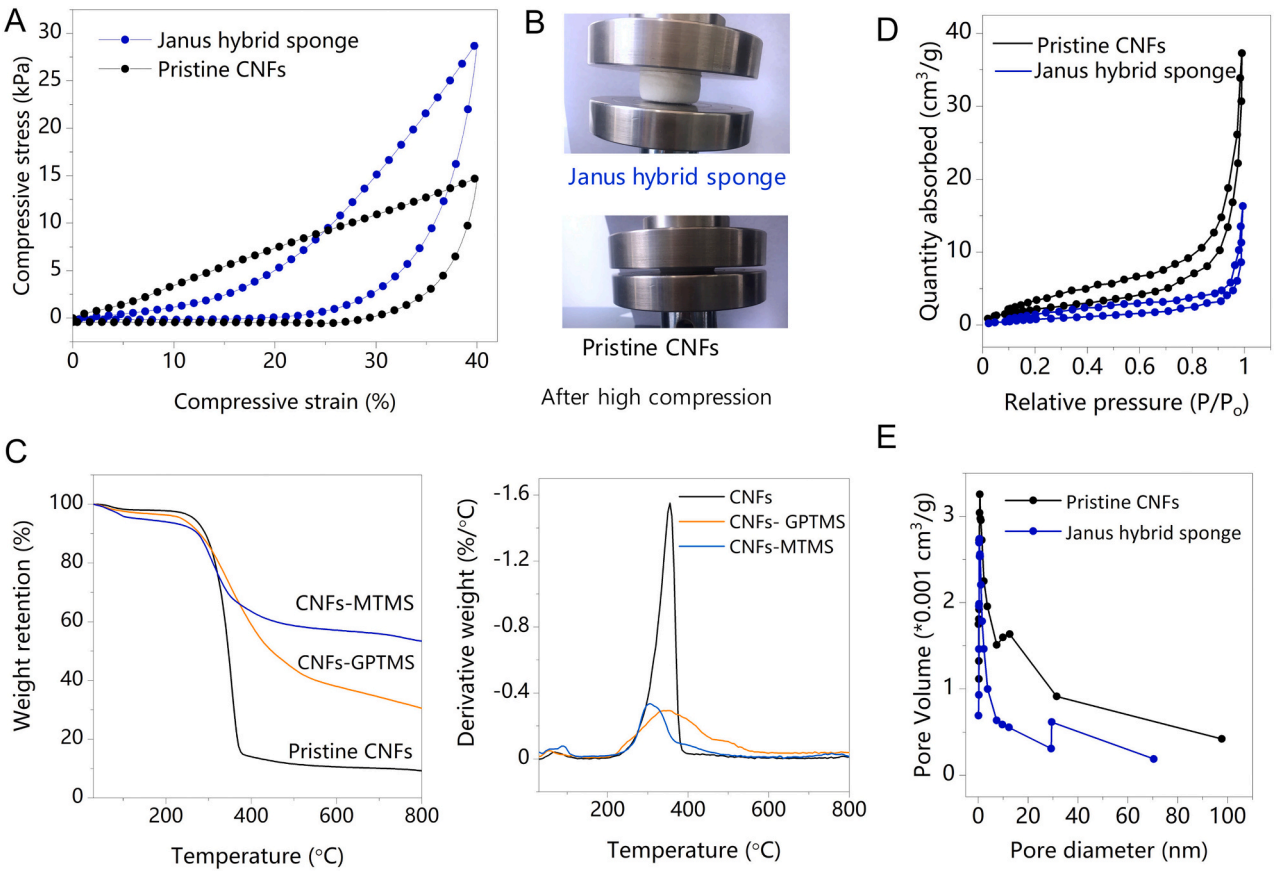

Fig. 3. Mechanical, thermal and porosity behaviors of Janus hybrid sponge. (A) Comparative compressive tress-strain behaviors of pristine CNF and Janus CNF sponge. (B) Photographic images of both the Janus hybrid sponge and pristine CNF after compression. (C) TGA curves of CNF GPTMS- and MTMS-modified CNFs in nitrogen atmosphere, together with their corresponding derivative TG. (D) Comparison of the N_2 adsorption-desorption isotherms and (E) pore size distribution of pristine CNF and Janus hybrid sponge.

region corresponds to elastic buckling and stretching of the cellulose cell walls. The intermediate strain area where the cell walls tend to fail and an abrupt stress increasing regime (high-strain region) corresponds to the densification of cells because opposite cell walls tend to come in contact with each other [30]. Moreover, the Janus hybrid sponge was stronger than the pristine CNFs in the densification regime with some differences observed in the initial compression stages ascribed to the different mechanisms of distributing stress in the sponges. The modified sponge has nanoparticles, nanofibers, and nanofilms which all take part in the efficient stress distribution within the sponge as opposed to the pristine CNF sponge. Overall, with 60% compressive strain, the Janus hybrid CNF sponge could take in 29 kPa of stress as compared to only 15 kPa for the CNF sponge. This is strongly attributed to the strong cross-linking effect, enabling good structural robustness. More still, the compression stress-strain curve demonstrated that the Janus hybrid sponge recovered almost back to its original shape (even after 80% strain, Fig. S4) of which neat CNF sponge could not, showing good mechanical properties (Fig. 3B). Therefore, due to excellent compressive elasticity, the Janus hybrid sponge can be regenerated and easily used through mechanically squeezing out of the oil (if used for spill cleaning).

3.1.5. *Thermal gravimetric analysis*

All the tested CNF sponges exhibited a three-step thermal gravimetric analysis (TGA) degradation profile (Fig. 3C). Generally, the initial weight loss ($T < 250$ °C) was attributed to dehydration or evaporation of adsorbed moisture without thermal degradation. The second degradation step starting from 250 °C to 400 °C is associated with accelerated weight loss and is attributed to oxidative decomposition of CNF chains. During a TGA measurement, it is expected that the silica content on the CNF and carbon will remain after 800 °C as silica is stable up to 1700 °C. From TGA data, we were able to determine higher amount of residue from GPTMS and MTMS modified samples, which also confirmed the presence of additional silica residue to ash in the modified CNFs as opposed to ash only in CNFs. More still, the increased presence of carbon yield and silica during thermolysis tends to facilitate the formation of a protective heat-resistant layer [31], capable of impeding the heat transport which as a result hampers the formation of flammable gases, consequently decreasing the amount of heat travelling around in modified CNFs (with MTMS and GPTMS), making them better candidates than pristine CNFs towards various high-temperature applications.

3.1.6. *Porosity analysis*

N_2 adsorption–desorption isotherms provided important details about the pore structures of pristine and modified CNF sponges (Fig. 3C). The Janus hybrid sponges displayed IV-type adsorption isotherm according to IUPAC classification and the evident adsorption-desorption hysteresis loops originating from capillary condensation. The pore size distribution (Fig. 3D) was in the range of 1–100 nm and 1–70 nm for the pristine CNF and Janus hybrid sponges, respectively. This indicates the presence of macropores (>50 nm mesopores (2–50 nm) and micropores (<2 nm)) [27,32]. The BET results indicated a much lower specific area for the Janus hybrid sponge (3.9 m^2/g) as compared with the pristine CNF sponge (8.5 m^2/g). Also, BJH results showed that the Janus hybrid sponge had a higher pore volume of 0.06 m^3/g as compared to 0.03 m^3/g from pristine CNF sponge. This can be attributed to the functionalization of CNFs in modified samples in which new molecules were deposited on CNFs, which resulted into the increased

density of the sponge, which overall decreased the specific surface area and increased the pore volume of the Janus hybrid sponge. More notably, we observed a steady suppression in BET surface area with increased MTMS or GPTMS content (not shown), signifying that the void volume fraction was suppressed within the sponge as a result of condensing of the cellulosic scaffold after silylation. Nevertheless, the Janus hybrid CNF sponge remained highly porous and light.

3.2. Application of all-CNF sponge in oil-water separation

3.2.1. Sorption efficiency of the sponges

In the next section we utilized the Janus hybrid CNF sponge in oil-water separation application. Preliminary tests were performed to determine the sorption efficiency of the sponges on several organic solvents (Fig. 4). Briefly, oil red was added to organic oil solvents (n-Hexane, toluene, dichloromethane (DCM), tetrahydrofuran (THF), and paraffin) and the mixture was sonicated to give a homogeneous oil solution. Then, 1 mL of dyed oil mixture was added to water (Fig. 4A). Then, the Janus hybrid sponge was placed in contact with oil-water mixture until the oil was completely absorbed on the hydrophobic side of the CNF sponge (Fig. 4B). The same procedure was repeated for sorption of other oil-water mixtures. After the absorption process, the Janus hybrid CNF sponge was immersed in ethanol for 1 h to reclaim the organic solvent. The absorption efficiency data is shown in Fig. 4B, with the Janus hybrid sponge showing excellent absorption efficiency for toluene. Generally, the oil absorption performance was rapid in about 30 s, which can be explained by the high porosity of the Janus hybrid sponge offering more porous channels for oil within the sponge. The flat shapes of the curves after 90s is ascribed to maximum absorption capacity the Janus hybrid CNF sponge when its surface area was almost occupied fully by absorbed oils, hence preventing the sponge from taking in extra oil. The maximum oil absorption capacity of the Janus hybrid sponge was achieved in less than 30 s for DCM. The performance observations of the Janus hybrid sponge are due to its effective pores and the 3D enhanced networked morphology facilitated by the crosslinkers. The high porosity gives huge storage space to the Janus hybrid sponge for oils and 3D morphology provides channels for oil to readily enter the interior of Janus hybrid sponge.

3.2.2. Unidirectional gravity-driven separation

For gravity-driven oil-water separation application, the CNF Janus hybrid sponge was placed between 2 glass tubes (d = 2 cm) with flange and fastened with a masking tape. The Janus hybrid CNF sponge was switched between hydrophilic side (Fig. 5A) and hydrophobic side (Fig. 5B) facing the oil-water feed. The oil-water mixture was separated from the upper to the lower tube. Fig. 5A shows the gravity-driven separation of water from water-oil emulsion with the Janus hybrid CNF sponge having its hydrophilic layer on the feed side of the oil-water mixture. In Fig. 5B, the orientation of the Janus hybrid CNF sponge was flipped with the hydrophobic side facing the feed. This is because the sponge could allow water to pass through (for hydrophilic side facing the feed) but repelling oil. The same with the hydrophobic side facing feed, which allowed oil to pass through but repelling water. In the earlier case (Fig. 5A), we could collect only pure water, and in the latter case (Fig. 5B) only oil. The optical microscope images before and after separation of water from oil-water mixture is shown in Fig. C. Here, the Janus hybrid CNF sponge acted as a switchable barrier courtesy of the observed two-faced properties on each side. Due to the asymmetric surface wettability, each side of the sponge performs individually during oil/water separation, and thus the Janus hybrid sponge demonstrates switch ability by facilely changing the oil-water mixture feed. A summary plot of the separation performance/permeate flux and their separation efficiency (in Fig. S5) with facile gravity-driven separation of oil-water emulsion using the Janus hybrid CNF sponge is provided in Fig. 5D, respectively. The general mechanism of separation goes as follows; in scenario one (Fig. 5A) where the hydrophilic layer of the Janus hybrid sponge is in contact with the feed of the oil-water mixture, the sponge allows continuous water phase flow through it. However, the rejected oil (if much) tends to accumulate and can easily form a barrier layer on the sponge surface impeding water penetration [33,34]. This is

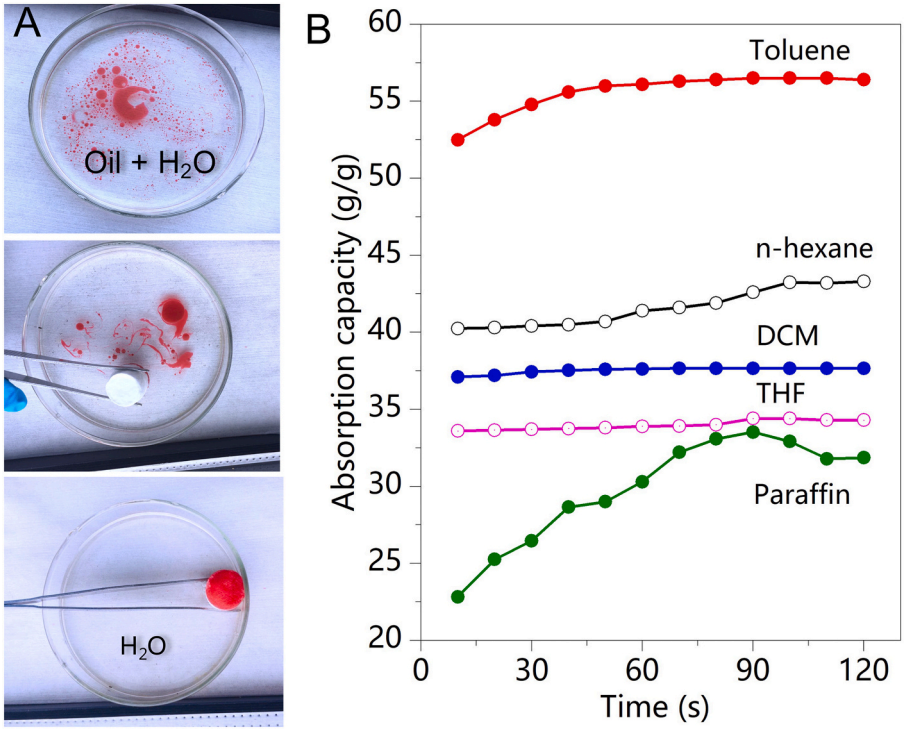

Fig. 4. Sorption of organic solvents. (A) Demonstration of the performance of Janus hybrid sponge towards removal of organic solvents from water. (B) A plot of the mass absorption kinetics depicting the absorption capacity across 120 s for different organic solvents.

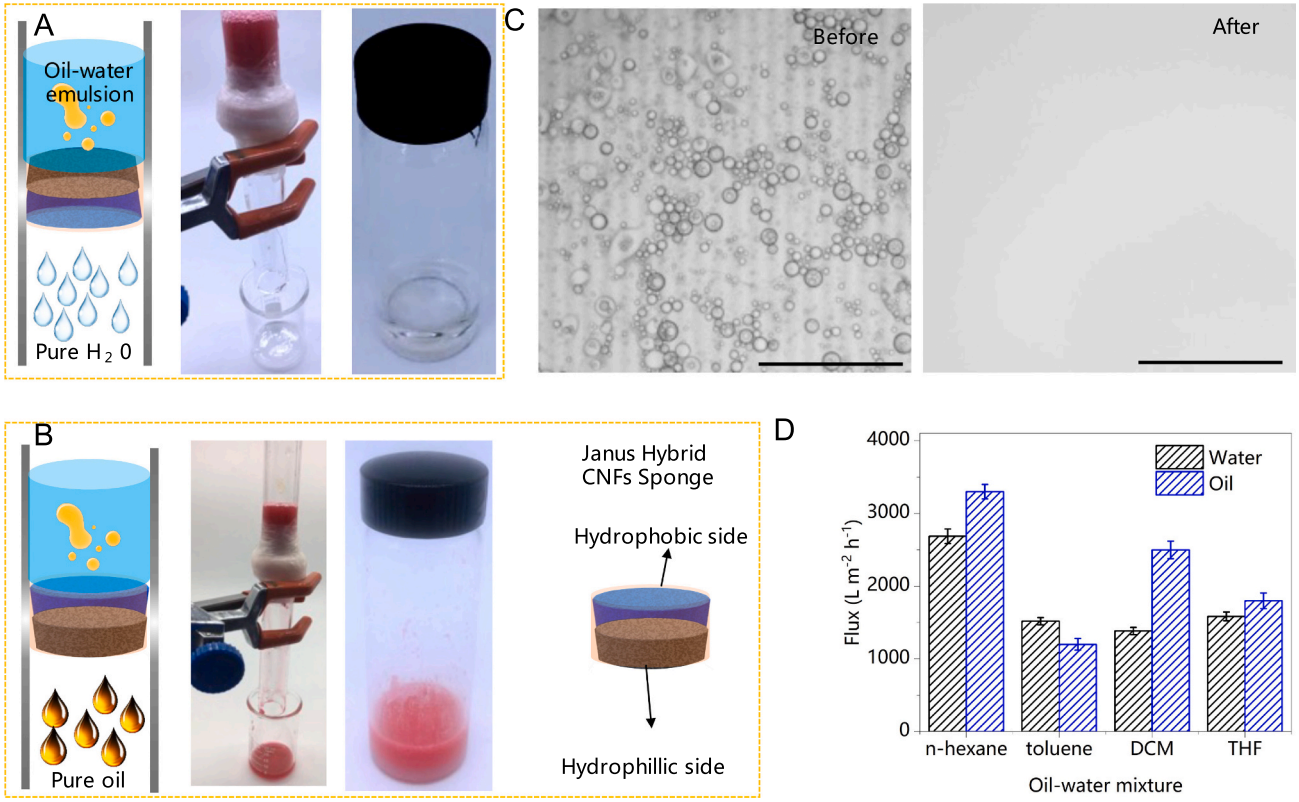

Fig. 5. Unidirectional gravity-driven Oil-water separation of Janus hybrid sponge. (A-B) Experimental setup depicting images for oil/water separation apparatus with a facile gravity-driven approach. The Janus hybrid CNF sponge has one side hydrophobic and opposite side hydrophilic. It was flipped opposite in B as compared to A. The water and oil flux obtained after filtration in A and B is shown in the bottles. (C) The optical microscope images show the oil-water mixture before and after separation. Scale bars are 60 μm (B) A plot of separation performance/permeate flux (oil or water) with facile gravity-driven separation of different oil/water emulsions using the Janus hybrid CNF sponge together.

the reason as to why we see the water flux decreasing when the concentration of oil in water is high (Fig. S6). The opposite is true when the Janus hybrid sponge is flipped exposing the hydrophobic side to the feed which allows the oil phase to flow through. This reason explains why the Janus hybrid sponge was very effective for the separation of low-viscosity oils (Fig. S7). At last, the reusability of the sponges was evaluated by rinsing the samples three times with 50 mL of ethanol for 10 min. More interestingly, the squeezed sample could quickly absorb oil again and regained most of its volume. We quantified the effectiveness of oil-water (water permeate) separation after 3 cycles with same sponge for n-hexane, toluene, DCM and THF emulsions. The performance of the sponge was 93, 53, 100, and 76% for n-hexane, toluene, DCM and THF emulsions, respectively (Fig. S8).

4. Conclusion

In summary, we have successfully demonstrated a facile and reproducible approach to fabricate and design Janus hybrid sustainable hybrid all-CNF sponge with asymmetric wettability by combining two differently modified CNF suspensions *via* freeze-shape drying approach, curing to further promote crosslinking. The process induced a superhydrophobic-superhydrophilic wettability with a water contact angle of up to 156°, super elasticity and high pore tortuosity. The Janus hybrid sustainable all-CNF sponge could effectively separate oil-water emulsions under gravity up to high flux values of 3300 L m^{-2} h^{-1} (oil flux) and 2687 L m^{-2} h^{-1} (water flux) by simple switching of Janus hybrid sponge faces. More still, our sponge exhibited superior anti-fouling property with ease in application. It is anticipated that such fabricated sponge can find applications in oil spill clean-up, fuel purification, wastewater treatment and many others.

CRediT authorship contribution statement

Aphra Agaba: Methodology; Data curation; Formal analysis; Investigation; Roles/Writing – original draft
Ifra Marriam: Writing – review & editing
Mike Tebyetekerwa: Conceptualization, Writing – review & editing
Wang Yuanhao: Conceptualization; Project administration; Resources; Validation; Supervision.

Declaration of competing interest

The authors declare that they have no known competing financial interests or personal relationships that could have appeared to influence the work reported in this paper.

Appendix A. Supplementary data

Supplementary data to this article can be found online at https://doi.org/10.1016/j.ijbiomac.2021.07.027.

References

[1] M. Liu, S. Wang, L. Jiang, Nature-inspired superwettability systems, Nat. Rev. Mater. 2 (7) (2017) 1–17, https://doi.org/10.1038/natrevmats.2017.36.
[2] Y. Liu, K. He, G. Chen, W.R. Leow, X. Chen, Nature-inspired structural materials for flexible electronic devices, Chem. Rev. 117 (20) (2017) 12893–12941, https://doi.org/10.1021/acs.chemrev.7b00291.
[3] T. Sun, G. Qing, B. Su, L. Jiang, Functional biointerface materials inspired from nature, Chem. Soc. Rev. 40 (5) (2011) 2909–2921, https://doi.org/10.1039/c0cs00124d.
[4] Ç.K. Söz, S. Trosien, M. Biesalski, Janus Interface materials: a critical review and comparative study, ACS Mater. Lett. 2 (4) (2020) 336–357, https://doi.org/10.1021/acsmaterialslett.9b00489.

[5] Z. Wu, L. Li, T. Liao, X. Chen, W. Jiang, W. Luo, J. Yang, Z. Sun, Janus nanoarchitectures: from structural design to catalytic applications, Nano Today 22 (2018) 62–82, https://doi.org/10.1016/j.nantod.2018.08.009.
[6] M. Nau, N. Herzog, J. Schmidt, T. Meckel, A. Andrieu-Brunsen, M. Biesalski, Janus-type hybrid paper membranes, Adv. Mater. Interfaces 6 (18) (2019) 1900892, https://doi.org/10.1002/admi.201900892.
[7] M. Zhang, L. Wang, Y. Hou, W. Shi, S. Feng, Y. Zheng, Controlled smart anisotropic unidirectional spreading of droplet on a fibrous surface, Adv. Mater. 27 (34) (2015) 5057–5062, https://doi.org/10.1002/adma.201502143.
[8] M. Lattuada, T.A. Hatton, Synthesis, properties and applications of janus nanoparticles, Nano Today 6 (3) (2011) 286–308, https://doi.org/10.1016/j.nantod.2011.04.008.
[9] R.K. Gupta, G.J. Dunderdale, M.W. England, A. Hozumi, Oil/water separation techniques: a review of recent progresses and future directions, J. Mater. Chem. A 5 (31) (2017) 16025–16058, https://doi.org/10.1039/c7ta02070h.
[10] Y. Deng, C. Peng, M. Dai, D. Lin, I. Ali, S.S. Alhewairini, X. Zheng, G. Chen, J. Li, I. Naz, Recent development of super-wettable materials and their applications in oil-water separation, J. Clean. Prod. 121624 (2020), https://doi.org/10.1016/j.jclepro.2020.121624.
[11] C. Chen, D. Weng, A. Mahmood, S. Chen, J. Wang, Separation mechanism and construction of surfaces with special wettability for Oil/Water separation, ACS Appl. Mater. Interfaces 11 (11) (2019) 11006–11027, https://doi.org/10.1021/acsami.9b01293.
[12] F. Ding, M. Gao, Pore wettability for enhanced oil recovery, contaminant adsorption and oil/water separation: a review, Adv. Colloid Interf. Sci. 289 (2021), 102377, https://doi.org/10.1016/j.cis.2021.102377.
[13] K. Lee, P. Stoffyn-Egli, G.H. Tremblay, E.H. Owens, G.A. Sergy, C.C. Guénette, R. C. Prince, Oil–mineral aggregate formation on oiled beaches: natural attenuation and sediment relocation, Spill Science & Technology Bulletin 8 (3) (2003) 285–296, https://doi.org/10.1016/S1353-2561(03)00042-2.
[14] R.d.C.F. Silva, D.G. Almeida, R.D. Rufino, J.M. Luna, V.A. Santos, L.A. Sarubbo, Applications of biosurfactants in the petroleum industry and the remediation of oil spills, Int. J. Mol. Sci. 15 (7) (2014) 12523–12542, https://doi.org/10.3390/ijms150712523.
[15] Q. Lin, I.A. Mendelssohn, K. Carney, S.M. Miles, N.P. Bryner, W.D. Walton, In-situ burning of oil in coastal marshes. 2. Oil spill cleanup efficiency as a function of oil type, marsh type, and water depth, Environ. Sci. Technol. 39 (6) (2005) 1855–1860, https://doi.org/10.1021/es0490626.
[16] A. Jaggi, J.R. Radovic, L.R. Snowdon, S.R. Larter, T.B. Oldenburg, Composition of the dissolved organic matter produced during in situ burning of spilled oil, Org. Geochem. 138 (2019), 103926, https://doi.org/10.1016/j.orggeochem.2019.103926.
[17] M. Fingas, The Basics of Oil Spill Cleanup, Third ed., CRC Press, Boca Raton, 2012.
[18] H. Liu, B. Geng, Y. Chen, H. Wang, Review on the aerogel-type oil sorbents derived from nanocellulose, ACS Sustain. Chem. Eng. 5 (1) (2017) 49–66, https://doi.org/10.1021/acssuschemeng.6b02301.
[19] V. Thakur, A. Guleria, S. Kumar, S. Sharma, K. Singh, Recent advancements in nanocellulose processing, functionalization and applications: a review, Materials Advances (2021), https://doi.org/10.1039/d1ma00049g.
[20] F. Liu, M. Ma, D. Zang, Z. Gao, C. Wang, Fabrication of superhydrophobic/superoleophilic cotton for application in the field of water/oil separation, Carbohydr. Polym. 103 (2014) 480–487, https://doi.org/10.1016/j.carbpol.2013.12.022.
[21] Z. Zhang, G. Sèbe, D. Rentsch, T. Zimmermann, P. Tingaut, Ultralightweight and flexible silylated nanocellulose sponges for the selective removal of oil from water, Chem. Mater. 26 (8) (2014) 2659–2668, https://doi.org/10.1021/cm5004164.
[22] F. Jiang, Y.-L. Hsieh, Amphiphilic superabsorbent cellulose nanofibril aerogels, J. Mater. Chem. A 2 (18) (2014) 6337–6342, https://doi.org/10.1039/c4ta00743c.
[23] S. Wang, X. Peng, L. Zhong, J. Tan, S. Jing, X.F. Cao, W. Chen, C. Liu, R. Sun, Ultralight, elastic, cost-effective, and highly recyclable superabsorbent from microfibrillated cellulose fiber for oil spillage cleanup, J. Mater. Chem. A 3 (16) (2015) 8772–8781, https://doi.org/10.1039/c4ta07057g.
[24] A.J. Svagan, M.A.S.A. Samir, L.A. Berglund, Biomimetic foams of high mechanical performance based on nanostructured cell walls reinforced by native cellulose nanofibrils, Adv. Mater. 20 (7) (2010) 1263–1269, https://doi.org/10.1002/adma.200701215.
[25] G. Chen, T. Chen, K. Hou, W. Ma, M. Tebyetekerwa, Y. Cheng, W. Weng, M. Zhu, Robust, hydrophilic graphene/cellulose nanocrystal fiber-based electrode with high capacitive performance and conductivity, Carbon 127 (2018) 218–227, https://doi.org/10.1016/j.carbon.2017.11.012.
[26] S. Zhou, M. Wang, X. Chen, F. Xu, Facile template synthesis of microfibrillated cellulose/polypyrrole/silver nanoparticles hybrid aerogels with electrical conductive and pressure responsive properties, ACS Sustain. Chem. Eng. 3 (12) (2015) 3346–3354, https://doi.org/10.1021/acssuschemeng.5b01020.
[27] Y. Jiao, C. Wan, T. Qiang, J. Li, Synthesis of superhydrophobic ultralight aerogels from nanofibrillated cellulose isolated from natural reed for high-performance adsorbents, Appl. Phys. A Mater. Sci. Process. 122 (7) (2016) 686, https://doi.org/10.1007/s00339-016-0194-5.
[28] H. Cheng, Y. Li, B. Wang, Z. Mao, H. Xu, L. Zhang, Y. Zhong, X. Sui, Chemical crosslinking reinforced flexible cellulose nanofiber-supported cryogel, Cellulose 25 (1) (2018) 573–582, https://doi.org/10.1007/s10570-017-1548-7.
[29] Z. Xue, S. Wang, L. Lin, L. Chen, M. Liu, L. Feng, L. Jiang, A novel superhydrophilic and underwater superoleophobic hydrogel-coated mesh for oil/water separation, Adv. Mater. 23 (37) (2011) 4270–4273, https://doi.org/10.1002/adma.201102616.
[30] H. Françon, Z. Wang, A. Marais, K. Mystek, A. Piper, H. Granberg, A. Malti, P. Gatenholm, P.A. Larsson, L. Wågberg, Ambient-dried, 3D-printable and electrically conducting cellulose nanofiber aerogels by inclusion of functional polymers, Adv. Funct. Mater. 30 (12) (2020) 1909383, https://doi.org/10.1002/adfm.201909383.
[31] Z.L. Yu, N. Yang, V. Apostolopoulou-Kalkavoura, B. Qin, Z.Y. Ma, W.Y. Xing, C. Qiao, L. Bergstrom, M. Antonietti, S.H. Yu, Fire-retardant and thermally insulating phenolic-silica aerogels, Angew Chem. Int. Ed. Engl. 57 (17) (2018) 4538–4542, https://doi.org/10.1002/anie.201711717.
[32] Z. Xu, F. Xie, J. Wang, H. Au, M. Tebyetekerwa, Z. Guo, S. Yang, Y.-S. Hu, M.-M. Titirici, All-cellulose-based quasi-solid-state sodium-ion hybrid capacitors enabled by structural hierarchy, Adv. Funct. Mater. 29 (39) (2019) 1903895, https://doi.org/10.1002/adfm.201903895.
[33] J. Wu, N. Wang, L. Wang, H. Dong, Y. Zhao, L. Jiang, Unidirectional water-penetration composite fibrous film via electrospinning, Soft Matter 8 (22) (2012) 5996–5999, https://doi.org/10.1039/c2sm25514f.
[34] Y.P. An, J. Yang, H.C. Yang, M.B. Wu, Z.K. Xu, Janus membranes with charged carbon nanotube coatings for deemulsification and separation of oil-in-water emulsions, ACS Appl. Mater. Interfaces 10 (11) (2018) 9832–9840, https://doi.org/10.1021/acsami.7b19700.